Proceedings of the XVII ECSMGE-2019
Geotechnical Engineering foundation of the future
ISBN 978-9935-9436-1-3

doi: 10.32075/17ECSMGE-2019-0390

XVII European Conference
ECSMGE 2019
Reykjavik
on Soil Mechanics
and Geotechnical Engineering

Soil-structure interaction in field pull-out tests of soil anchors and additional resistance from the reaction plate

Interaction sol-structure lors d'essais d'arrachement sur le terrain des ancrages de sol et résistance supplémentaire due à la réaction

H. J. Seo
Xi'an Jiaotong-Liverpool University, China

G. Marketos
Tony Gee and Partners LLP, Esher, UK
L. Pelecanos
University of Bath, Bath, UK

ABSTRACT: Soil anchors are used to stabilise soils and provide additional support to earth retaining structures. In-situ pull-out tests can be performed in the field to provide information about the anchor capacity. An anchor is installed in the ground and a tensile force is applied at the base of the anchor. To apply this tensile force, a steel "reaction plate" is installed at the ground surface which is vertically loaded. Instrumentation provides information about the axial strains and further data processing provides information about the mobilised skin friction. Recent field tests have shown evidence of soil-structure interaction in the ground close to the reaction plate, which provides additional resistance. This may imply that the test results may have some degree of uncertainty and their interpretation may lead to overprediction of the true capacity and therefore unconservative designs. This paper presents high quality monitoring data from a anchor pull-out test. Data analysis shows the effect of the reaction plate in enhancing the observed capacity of the anchor. Complementary numerical analyses, both load-transfer (t-z) and 2D axisymmetric solid finite element analysis, are performed in order to quantify the effect of this reaction plate.

RÉSUMÉ: Les tests d'ancrage dans le sol sont modélisés avec des éléments finis. Le plateau de réaction en acier offre une résistance supplémentaire. Les données de test sur le terrain sont comparées aux analyses par éléments finis.

Keywords: soil anchors, soil-structure interaction, pull-out tests, finite element analysis, reaction plate

1 INTRODUCTION

Soil anchors are widely used to provide support to earth retaining structures and also assist in the control of displacements of retaining walls. They provide additional resistance to structural movements by mobilising the available pre-stress. The pre-stress is provided from enhancing the shear resistance of soil and the skin friction at the interface between the grout material and the surrounding soil. A critical component of the capacity of soil anchors is the interface shear strength between the grout and the surrounding soil (Tagaya et al., 1988; Powell & Watkins,

1990, Kumar & Kouzel, 2008). Several field tests and laboratory experiments can be carried out to derive the shear resistance between the grout and the soil. A widely used field technique is the pull-out test (Merrifield & Sloan, 2006; White et al., 2008; Seo et al., 2011a, 2017).

The interface resistance of a soil-nail and the soil mass is very complicated due to the combination of shear banding development at the nail-soil interface, hoop stresses around the circumference of the nail and confining pressure development with the depth (Seo et al., 2012, 2014a, b). In cases of a hybrid soil-nail and compression anchor system, the behavior mechanisms are even more complicated (Seo et al., 2010, 2011b) as the response is dictated by both a nail compression and an anchor tension. Extensive experimental and numerical research (Seo et al., 2016) is required to achieve an detailed understanding of the problem.

This study uses numerical models using both load-transfer and finite element analysis. Similar work was conducted earlier in distributed fibre optic sensing (Soga et al., 2015, 2017; Kechavarzi et al., 2016, 2019; Di Murro et al., 2016, 2019; Acikgoz et al., 2016, 2017) and was applied to monitoring axially-loaded piles (Ouyang et al., 15; Pelecanos et al., 2016, 2017a,b, 2018) and heat-exchanger foundation piles (Ouyang et al., 2018a,b,c).

This paper aims to quantify the additional resistance provided by a reaction plate on anchor pull-out tests. New data from a field test in Korea are presented and complemented by relevant load-transfer analysis and finite element (FE) simulations. The 2D axisymmetric FE simulations clearly illustrate the additional resistance provided by the steel reaction plate.

2 FIELD TESTS

A pull-out field test of an anchor was performed in Seoul, Korea. The examined pre-stressed concrete (PC) strands were made of steel with a diameter of 12.7 mm and 3 m long. The ground anchor consisted of two PC strands within plastic pipes, and an anchor body. The maximum yield load of two PC strands was 318 kN. The PC strands were located in a plastic pipe which was filled with oil so that no significant friction was developed between two PC strands and the plastic pipes when the PC strands were pulled. Consequently, the applied pull-out load was transferred directly to the anchor body, and therefore the anchor body could apply a stress on the grout material. To measure this load development within the grout, vibrating wire strain gauges (VWSGs) (SG4150 manufactured by GTC cooperation) were deployed using steel wires to fix on an auxiliary steel bar. A total of seven VWSGs were installed along the bar with some discrete intervals.

The anchor pull-out load was increased progressively and the developed strain values from the VWSGs at 4 load steps (40, 70, 100, 130kN) were recorded, as shown in Figure 1. Figure 1 (a) shows the profiles of axial force, whereas (b) the profiles of anchor skin friction. Axial force was calculated by multiplying the monitored axial strains by the axial rigidity, EA, (E is the anchor's Young's modulus and A is anchor cross-sectional area). The values of skin friction were calculated by differentiating the values of calculated axial strain with the depth. It may be observed that the values of axial force and skin friction increase gradually with the applied load. As anticipated, larger values of both axial force and skin friction occur close to the bottom of the anchor, which is nearer to the point of action of the load.

However, there are some unexpected non-zero axial force (i.e. axial strain) values at the top of the anchor, as the top of the anchor is free and therefore it would be expected to have zero strains. This suggests that there must be some additional soil resistance which is probably generated from the steel reaction plate at the ground surface. In order to further investigate this, complementary numerical analyses are performed in the following sections.

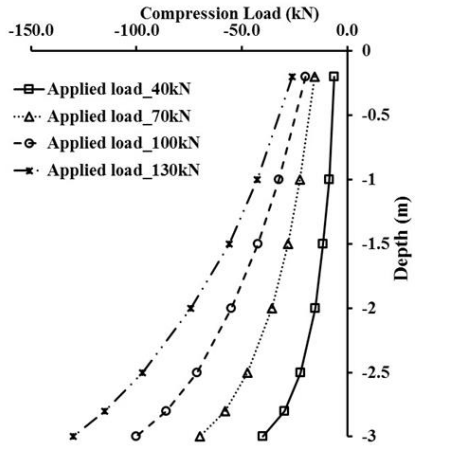

(a)

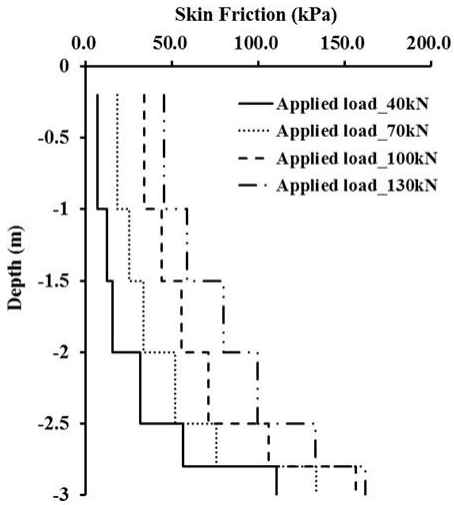

(b)

Figure 1. Field test results: (a) anchor top load-displacement curve, (b) profiles of axial anchor force and (c) profiles of anchor skin friction.

3 LOAD-TRANSFER MODELLING

3.1 The beam-spring model

The load-transfer computational model is based on a finite-element (FE) beam-spring formulation in which the anchor is simulated with two-noded beam elements with axial displacement degrees-of-freedom, whereas the soil is modelled with nonlinear springs, again with one degree-of-freedom, as shown in Figure 2.

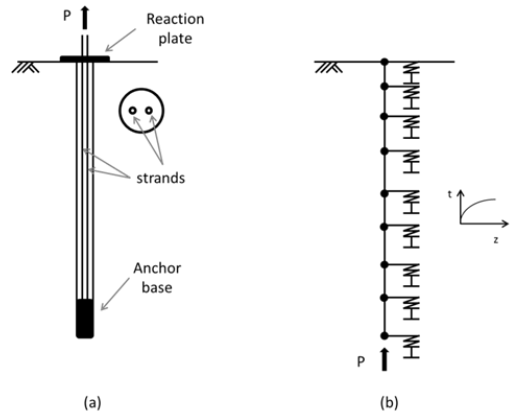

Figure 2. Load-transfer modelling: (a) an anchor pull-out field test and (b) a relevant finite element beam-spring model.

The governing FE equation (described by Equation 1) is global equilibrium and the global stiffness matrix comprises of the anchor stiffness matrix, $[K_a]$, and the soil stiffness matrix, $[K_s]$. Applied loads are added at the bottom of the anchor and define the load vector, {P}, whereas the solution of the equation provides the vector of vertical nodal displacements, {u}.

$$([K_a] + [K_s]) \cdot \{u\} = \{P\} \qquad (1)$$

The soil springs adopt a nonlinear load-transfer curve (t-z) defined by a hyperbolic-type relation, according to Equation 2. This equation provides the relation between shaft friction, t, with the local nodal displacement, z. It is a 4-parameter equation where t_m and k_m are related to the maximum value of friction and initial soil stiffness respectively. Lastly, the two dimensionless parameters d and h are related to stiffness degradation and hardening/softening respectively (Pelecanos & Soga, 2017a,b; 2018a,b).

$$t = \frac{k_m \cdot z}{\sqrt[d]{\left[1+\left(\frac{k_m}{t_m} \cdot z\right)^{(h \cdot d)}\right]}} \qquad (2)$$

The parameters of the load-transfer model were obtained from standard geotechnical pile stiffness (Randolph & Wroth, 1978) and capacity relations (Pelecanos et al., 2018). Table 1 presents the back-calculated parameters of the load-transfer model that were used in the FE analysis.

Table 1. Parameters of the load-transfer model.

Parameter Unit	k_m [kN/m^3]	t_m [kPa]	d []	h []
Value	22500	42	1	1

3.2 Results of the beam-spring model

The results of the load-transfer analysis are shown in Figure 3 and compared with the observed field data. Figure 3 (a) presents the profiles of vertical anchor nodal displacement, whereas (b) the profiles of the anchor skin friction (noted as the "original" model). It may be observed that there is a very good agreement between the field observed data and the computational predictions from the employed load-transfer model. This may prove that the derived load-transfer curves are suitable for modelling axial displacements, deformations and the ultimate response of such soil anchors.

It is also observed that there is a small mismatch between the numerical predictions of axial anchor force and those monitored during the field test, particularly closer to the top of the anchor. In particular, it is shown that the FE model predicts zero values of axial force at the top boundary. These zero values from the FE model were anticipated, as the boundary condition at the top of the anchor is free and therefore the stress should be equal to zero. It is expected that the non-zero values of axial force from the field data are due to the existence of the stiff steel reaction plate at the top of the anchor, at the ground surface, which has yielded some plate-soil-anchor interaction. Nevertheless, this observed difference however is moderately small and therefore negligible.

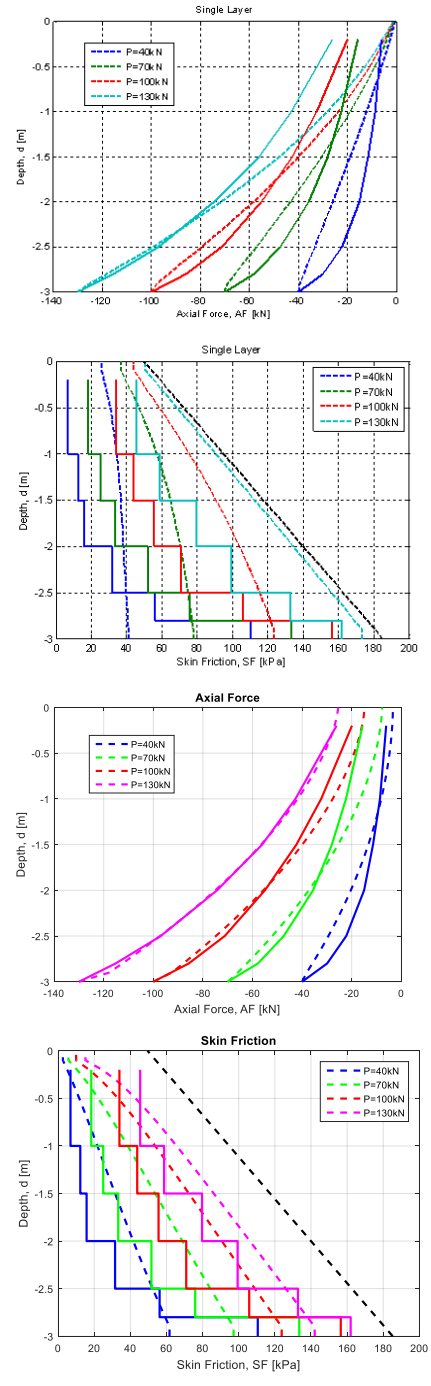

Figure 3. Results of finite element analysis: (a) profiles of vertical displacement [original model], (b) profiles of skin friction [original model], (c) profiles of vertical displacement [updated model] and (d) profiles of skin friction [updated model].

In order to overcome this mismatch in the axial force profiles close to the ground surface, an "updated" model was run, in which an additional vertical (axial) spring was added at the top of the ground anchor. This was done to accommodate for the presence of the reaction plate at the ground. Its stiffness parameters were obtained through a small parametric study in which the top displacements were assessed to be similar to those from the field test.

Figure 3 (c) presents the profiles of vertical anchor nodal displacement, whereas (d) the profiles of the anchor skin friction, both from the "updated" model. It may be observed that there is a very good agreement between the field observed data and the computational predictions from the employed load-transfer model. This may prove that the derived load-transfer curves are suitable for modelling axial displacements, deformations and the ultimate response of such soil anchors.

4 FINITE ELEMENT ANALYSIS

4.1 The Finite Element model

Subsequently, a finite element analysis of the problem was run using Plaxis 2D version 2018.0 in which it was possible to explicitly model the plate. Two cases were analysed so as to visualise the effect of the reaction plate and confirm the hypothesis that it has a measurable effect on the anchor pull-out test results: (I) The anchor was pulled out without the use of a reaction plate (and so any anchor-plate reaction is ignored) and, (II) the reaction plate (and the applied load on its surface) was fully modelled as described below.

The model was analysed in 2D axisymmetric conditions using the geometry shown in Figure 4. Note that due to the radial symmetry the 2D axisymmetric model is fully equivalent to a 3D model in which the 2D slice modelled is revolved by 360° around the r=0 axis (the left vertical boundary). A linear elastoplastic Mohr Coulomb constitutive model was used to represent the soil on site, with the material parameters given in Table 2. The anchor itself was modelled as a solid volume with the material properties of steel (linear elastic). The rectangular reaction plate was modelled with a stiff plate element and was idealised as an equivalent disc (circular) and therefore an equivalent radius for it was used in the axisymmetric model. The pullout force at the top of the anchor was included as an applied stress at the top surface of the anchor solid volume, while in the simulations where the reaction plate was included, a uniform downwards stress at the top of the reaction plate was modelled. The integration of the stresses at each surface is equal to the applied force on the anchor at each stage of the simulation (i.e. the downwards force applied at the reaction plate is equal to the upwards force on the anchor body). In order to allow for free movement of the anchor relative to the plate, the stiff anchor plate in the Plaxis model was terminated at a distance of 75mm from the anchor, i.e. there was an annular region of 75mm width around the anchor top surface over which the soil was more free to move. The width of this region was chosen to match the configuration of the field tests.

Figure 4. The axisymmetric FE model.

In Figure 4 the grey is the anchor volume, the blue line at the top surface is the reaction plate over which the downwards load is applied, and the green line is the annular area over which the soil is more free to move. Note that due to the radial symmetry the 2D axisymmetric model is fully equivalent to a 3D model in which the 2D slice modelled is revolved by 360° around the r=0 axis (the left vertical boundary).

Table 2. Material parameters of the FE model.

Material	γ_b kN/m^3	φ' deg	c' kPa	ψ deg	ν -	E MPa	Ko -
Soil	18.4	42.5	57.9	13		52	0.46
Anchor	18.4	-	-	-	-	200	-

4.2 Finite Element model results

The results of the FE analyses for both cases considered are shown and discussed in this section. Figure 5 shows the force versus displacement curves for both models run. As can be observed, the reaction plate stiffens the pullout response, even for the simplified Mohr-Coulomb analysis runs. Note that here we did not try to calibrate the soil input parameters so as to match the force displacement curve observed in the field. Invariably, a good match would also require the use of a nonlinear soil model. Nevertheless the results shown here are in our opinion very useful as they confirm the hypothesis of the effect of the plate, and as shown through Figures 6 and 7 help visualise what the effect of the reaction plate is.

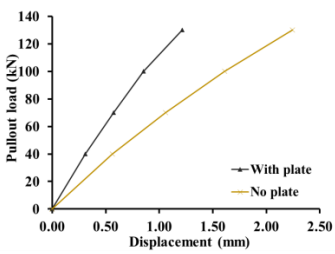

Figure 5. The pullout force versus displacement result for the Finite Element simulations. Results for a simulation that includes the reaction plate and for a simulation that does not.

Figure 6 shows the contours of horizontal stress within the soil for the no plate simulation, and the reaction plate simulation. It is shown that when ignoring the reaction plate at the ground surface the horizontal stresses are much smaller at the higher parts of the anchor, compared to the latter case that considers the reaction plate. This is perhaps expected, as the reaction plate results in higher confining stresses around the soil anchor there. This therefore increases the (drained) soil shear strength at that region and therefore results in more resistance from the ground, leading to a stiffer response. Note that some of the larger horizontal stresses in the lower parts of the anchor can be attributed to the fact that the dilation angle was 13°; dilation at a confined area of shearing, and the associated volume changes will lead to such an increase. This dilation however is driven by displacement magnitudes and so is also expected to occur for the simulation with the plate at higher anchor pullout displacements.

(a)

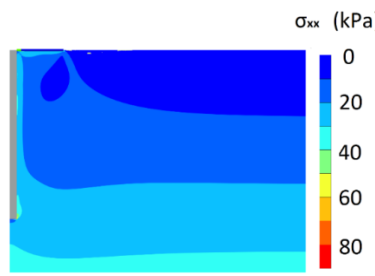

(b)

Figure 6. Predictions of the FE model for an anchor pullout force of 130kN: horizontal stress in the ground (a) Case I: no reaction plate, (b) Case II: with reaction plate.

5 CONCLUSIONS

The interaction behavior between soil anchors and the surrounding soil is a complicated phenomenon and still an unresolved engineering challenge. This is true because the soil-structure interaction is governed by a number of different mechanisms, such as the confining stress with the depth, the development of hoop stresses and the interaction with the test reaction plate.

This study investigates the effects of the reaction plate at the ground surface. Field test data are analysed and processing obtaining profiles of axial strain and skin friction. This is complemented by numerical analyses following two different approaches: load-transfer analysis and finite element analysis.

It is shown that the reaction plate creates some non-zero axial strains at the top of the soil anchor and some additional soil stresses. The numerical models that ignore or consider the presence of the reaction plate confirm that it results in additional stresses within the soil that may enhance the capacity performance of the soil anchor.

6 ACKNOWLEDGEMENTS

The Authors would like to acknowledge the assistance of the technicians and other colleagues in the field tests.

7 REFERENCES

Acikgoz, MS, Pelecanos, L, Giardina, G, Aitken, J & Soga, K 2017, 'Distributed sensing of a masonry vault during nearby piling', *Struct Control Health Monitoring*, **24**, e1872.

Acikgoz, MS, Pelecanos, L, Giardina, G & Soga, K 2016, 'Field monitoring of piling effects on a nearby masonry vault using distributed sensing.', *ICSIC*, ICE, Cambridge.

Di Murro, V, Pelecanos, L, Soga, K, Kechavarzi, C, Morton, RF & Scibile, L 2016, 'Distributed fibre optic long-term monitoring of concrete-lined tunnel section TT10 at CERN.', *ICSIC*, ICE, Cambridge.

Di Murro, V, Pelecanos, L, Soga, K, Kechavarzi, C, Morton, RF, Scibile, L, 2019, Long-term deformation monitoring of CERN concrete-lined tunnels using distributed fibre-optic sensing., *Geot Engineering* SEAGS. **50**.

Kechavarzi, C, Soga, K, de Battista, N, Pelecanos, L, Elshafie, MZEB & Mair, RJ 2016, *Distributed Fibre Optic Strain Sensing for Monitoring Civil Infrastructure*, ICE.

Kechavarzi, C., Pelecanos, L., de Battista, N., Soga, K. 2019. Distributed fiber optic sensing for monitoring reinforced concrete piles. *Geot Engineering* SEAGS. **50**

Kumar, J. and Kouzer, K.M., 2008. Vertical uplift capacity of horizontal anchors using upper bound limit analysis and fi-nite elements. Can Geot Journal, 45 698-704.

Merifield, R. S. and Sloan, S. W. (2006). “The ultimate pullout capacity of anchors in frictional soils.” Can Geot J, 43, 852–868.Ouyang, Y, Broadbent, K, Bell, A, Pelecanos, L & Soga, K 2015, 'The use of fibre optic instrumentation to monitor the O-Cell load test on a single working pile in London', *XVI ECSMGE*, Edinburgh.

Ouyang, Y., Pelecanos, L., Soga, K. 2018a, Thermo-mechanical response test of a cement grouted column embedded in London Clay, *Geotechnique* (Under Review).

Ouyang, Y., Pelecanos, L., Soga, K. 2018b, ‘Finite element modelling of thermo-mechanical behaviour and thermal soil-structure interaction of a thermo-active cement column buried in London Clay’. 9th *NUMGE*, Porto.

Ouyang, Y., Pelecanos, L., Soga, K. 2018c, ‘The field investi-gation of tension cracks on a slim cement grouted column’. *DFI-EFFC* Rome, Italy.

Pelecanos, L, Soga, K, Hardy, S, Blair, A & Carter, K 2016, 'Distributed fibre optic monitoring of tension piles under a basement excavation at the V&A museum in London.', *ICSIC*, Cambridge.

Pelecanos, L., Skarlatos, D. and Pantazis, G., 2017a. Dam per-formance and safety in tropical climates – recent develop-ments on field monitoring and computational analysis. *8th ICSECM*, Kandy, Sri Lanka.

Pelecanos, L, Soga, K, Chunge, MPM, Ouyang, Y, Kwan, V, Kechavarzi, C & Nicholson, D 2017b, 'Distributed fibre-optic monitoring of an Osterberg-cell pile test in London.', *Geotechnique Letters*, **7**, 1-9.

Pelecanos, L., Soga, K., Elshafie, M., Nicholas, d. B., Kechavarzi, C., Gue, C. Y., Ouyang, Y. and Seo, H., 2018. Distributed Fibre Optic Sensing of Axially Loaded Bored Piles. *J Geot Geoenv Eng*, **144**, 04017122.

Pelecanos, L., & Soga, K. 2017a. Innovative Structural Health Monitoring Of Foundation Piles Using Distributed Fibre-Optic Sensing. *8th ICSECM*, Kandy, Sri Lanka.

Pelecanos, L., & Soga, K. 2017b. The use of distributed fibre-optic strain data to develop finite element models for foundation piles. *6th FOSMG*, Nanjing, China.

Pelecanos, L & Soga, K 2018a, 'Using distributed strain data to evaluate load-transfer curves for axially loaded piles', *J Geot Geoenv Eng*, (Under Review).

Pelecanos, L., Soga, K. 2018b, 'Development of load-transfer curves for axially-loaded piles based on inverse analysis of fibre-optic strain data using finite element analysis and op-timisation'. *9th NUMGE. Porto*

Seo, H.J., Kim, H.R., Jeong, N.S. and Lee, I.M., 2010. Behavioral Mechanism of Hybrid Model of Soil-nailing and Compression Anchor. *J Korean Geot Soc*, **26** 117-133.

Seo, H.J., Jeong, K.H., Choi, H. and Lee, I.M., 2011a. Pullout resistance increase of soil nailing induced by pressurized grouting. *J Geot Geoenv Eng*, **138**.604-613.

Seo, H.J., Lee, G.H., Park, J.J. and Lee, I.M., 2012. Optimization of Soil-Nailing Designs Considering Three Failure Modes. J Korean Geot Soc, 28.5-16.Seo, H.J., Kim, H.R., Jeong, N.S., Shin, Y.J. and Lee, I.M., 2011b, December. Behavior of hybrid system of soil-nailing and compression anchor. *14th ARCSMGE*.

Seo, H.J. and Lee, I.M., 2014a. Shear Behavior between Ground and Soil-Nailing. *J Korean Geot Soc*, **30**, 5-16.

Seo, H.J., Lee, I.M. and Lee, S.W., 2014b. Optimization of soil nailing design considering three failure modes. *KSCE J of Civ Eng* , **18** 488-496.

Seo, H.J., Choi, H. and Lee, I.M., 2016. Numerical and exper-imental investigation of pillar reinforcement with pressurized grouting and pre-stress. TUST, 54,135-144.Seo, H., Pelecanos, L., Kwon, Y.S. and Lee, I.M., 2017. Net load-displacement estimation in soil-nailing pullout tests. *ICE Geot Eng*. **170** 534-547

Seo, H. J., Pelecanos, L., 2017. Load transfer in soil anchors – Finite Element analysis of pull-out tests. *8th ICSECM*, Sri Lanka.

Soga, K, Kechavarzi, C, Pelecanos, L, de Battista, N, William-son, M, Gue, CY, Di Murro, V & Elshafie, M 2017, 'Distributed fibre optic strain sensing for monitoring under-ground structures - Tunnels Case Studies ', in S Pamukcu, L Cheng (eds.), Underground Sensing, 1st edn, Elsevier.

Soga, K, Kwan, V, Pelecanos, L, Rui, Y, Schwamb, T, Seo, H & Wilcock, M 2015, 'The role of distributed sensing in un-derstanding the engineering performance of geotechnical structures', *XVI ECSMGE*, Edinburgh.

Tagaya, K., Scott, R.F. and Aboshi, H., 1988. Pullout resistance of buried anchor in sand. Soils and Foundations, 28 114-130.

White, D.J., Cheuk, C.Y. and Bolton, M.D., 2008. The uplift resistance of pipes and plate anchors buried in sand. Géotechnique, 58 771-779.